Localization For 5G MIMO Using Beam Switching and Channel Estimation

A School Project for COMP 5900, 5G Networks, Carleton University

Students: Charles Chen and Nicolas Perez
Course Instructor: Jun Huang

November 11, 2022

Abstract

5G MIMO technology has characteristics that are very favorable for performing localization. This project focuses on a previous work in 5G MIMO localization. Additional analysis of the previous work's performance is provided herein by varying the number of antenna elements, the transmitted frequencies and beamformers used. The original work is augmented using a beam switching technique to improve the localization and possibly simulate a real-world scenario which additionally involves high quality communications via a beamformer. This document also serves as a gentle introduction and tutorial to 5G localization, as it provides a documented Python implementation of the algorithms discussed herein, along with explanations of their prerequisite concepts.

Key words and phrases. 5G, MIMO, localization, beamforming, RSS, channel estimation, tutorial.

Contents

1 Introduction **5**
- 1.1 Why Use 5G for Localization? . . . 5
- 1.2 Purpose . . . 6
- 1.3 Scope . . . 7
- 1.4 5G Localization Tutorial . . . 7
  - 1.4.1 Related Documents . . . 8
  - 1.4.2 Angle of Arrival (AoA) . . . 8
  - 1.4.3 Angle of Departure (AoD) . . . 8
  - 1.4.4 Time of Arrival (TOA) . . . 8
  - 1.4.5 Gain . . . 8
  - 1.4.6 Friis Transmission Equation . . . 10
  - 1.4.7 Received Signal Strength (RSS) . . . 10
  - 1.4.8 Uniform Linear Array (ULA) . . . 12
  - 1.4.9 Representing Signals Using Complex Numbers . . . 12
  - 1.4.10 Complex Gain . . . 13
  - 1.4.11 Subcarriers . . . 13
  - 1.4.12 Array Response Vectors . . . 13
  - 1.4.13 Channel Model . . . 16
  - 1.4.14 Beamforming . . . 17
  - 1.4.15 Received Signal Model . . . 21
  - 1.4.16 Localization Using Channel Estimation . . . 21
  - 1.4.17 Localization Using Beam Switching . . . 22
- 1.5 Application . . . 23

2 Functional Overview **23**
- 2.1 System Overview . . . 23
- 2.2 Assumptions . . . 24
  - 2.2.1 Antenna Hardware . . . 24
  - 2.2.2 Mobile Station Velocity . . . 24
  - 2.2.3 Line of Sight . . . 24

3 Detailed Functional Descriptions **25**
- 3.1 Channel Estimation Localization . . . 25
  - 3.1.1 Algorithm . . . 25

3.1.2 Results 27
3.2 Combining Channel Estimation Localization and Beam Switching Localization 28
3.2.1 Algorithm 28
3.2.2 Results 31

4 Conclusion **32**
4.1 Discussion on Previous Localization Work 32
4.2 Ideas for Future Work 33

5 Appendices **33**
5.1 Change Log 33
5.2 Code 33
5.3 Contributions 34
5.3.1 Charles Chen's Contributions 34
5.3.2 Nicolas Perez's Contributions 34

1 Introduction

1.1 Why Use 5G for Localization?

5G is most commonly thought of as a form of communication. However, the same radio access network (RAN) that enables wireless communication can also provide accurate localization. Before gettong into the details of our project, we will explain why 5G should be considered for applications requiring localization. The following characteristics are what make 5G an effective technology for localization [1, 2]:

1. Massive MIMO (multiple-input multiple-output) devices are devices that have a large number of antennas (more specifically refferred to as antenna elements) placed closely together (usually less than a centimeter a part). Communication using multiple antenna elements at either the BS (base station) and/or MS (mobile station) cause the characteristics of the channel between the BS and MS to be highly dependent on their relative orientation to one another. Thus, received signals can be 'reverse engineered' to reveal the relative orientation of the BS and MS. These antenna configurations are most commonly used to focus transmit and receive signals in a specific direction(s) via beam forming to improve the quality of communications. The quality of a signal is characterized by its SINR (signal-to-noise-plus-interference) value, where higher values (which means a higher quality signal) equates to more accurate relative orientation estimation. The more antennas used, the better the orientation estimation (the word 'massive' in massive MIMO means 'many antennas').

2. Higher frequencies translates to shorter wavelengths, which in turn allows for more tightly packed antenna elements, thus enabling massive MIMO. Beamforming requires spacing between antenna elements to be proportional to the wavelength of the signal. Higher frequencies also result in fewer multipath components. Multipath propagation is when multiple copies of a signal arrives at the receiver due to the signal bouncing off, refracting through or diffracting around a substance. At higher frequencies, the receiver will typically receive less copies of the same signal than if it were transmitted us-

ing a lower frequency. This makes the localization process easier as there all less copies of the same signal that may cause interference or increase the complexity of the problem (i.e. identifying and tracking copies of the same signal). Moreover, high frequency signals that are received by the receiver due to multipath can be assumed to be from a single bounce, further simplifying the problem.

3. Larger bandwidths equates to lower delay in communication, as length (in terms of time) of symbols (the units of data that are transmitted wirelessly) can be shortened. Low delay is important in applications with high safety requirements, for example, autonomous vehicle control. The larger bandwidths also allow for a finer resolution when measuring time differences, a fundamental component to accurate positioning algorithms. Finally, higher bandwidth allows easier identification of multipath components.

4. D2D (device to device) 5G communications is ultra-fast and highly reliable. D2D communication enables cooperative localization, where devices not only localize by communicating with BSs, but also by calculating relative positions between one another.

5. Network densification, a common characteristic of 5G networks that entails base stations having overlapping coverage areas, can further enhance localization. By combining measurements from multiple BSs, accuracy and reliability of localization can be improved. Additionally, with more BSs in range of a device there is a higher likelihood of one of the BSs having LOS (line of sight) to the MS. Having LOS means the straight line path that passes through the BS and the MS is free of physical obstructions that would stop a signal travelling along that path.

1.2 Purpose

The purpose of this project is to explore 5G localization techniques and provide a concise explanation of its core prerequisite concepts. In our process of exploring 5G localization techniques, we thought of a way to combine beamforming, RSS (received signal strength) measurements, and

a known localization algorithm. The implementation of this method also illustrates a realistic 5G scenario that involves localization as well as beamforming (the latter of which may be used for communication). Thus, it also explores the synergy between localization and communication.

1.3 Scope

This document assumes the reader has very little prior knowledge about 5G localization, and some basic knowledge about 5G in general. Beamforming and the geometry-based 5G channel model, [3], ubiquitously used in 5G localization techniques, will be explained. General localization concepts will also be explained. See subsection 1.4 for an explanation of the previously listed prerequisite concepts for understanding 5G localization. The application of 5G localization techniques is briefly reviewed in subsection 1.5.

Section 2 gives a high-level outline of the implemented algorithms related to this document, as well as some assumptions we made about the environment and hardware our algorithms operate under. Section 3 will go into a more detailed description of the algorithms. Section 4 will discuss the results in this document, along with a conclusion and discussion of what has been established. Section 5 will give a reference to this document's associated implementation as well as a brief description of its usage. It will also outline the contributions each author has made in this project.

1.4 5G Localization Tutorial

This subsection serves as a 'tutorial' on localization using 5G. It explains in detail the prerequisite concepts for understanding 5G localization algorithms. As far as we are aware, this is the most extensive and descriptive work on the prerequisite knowledge needed to understand the mathematics and concepts used in 5G localization techniques. We hope that it is useful to you!

We assume that the reader understands first year university level linear algebra, high school level trigonometry, complex numbers, and knows

how to take the magnitudes and conjugates of complex numbers and complex vectors. Typically a basic model consisting of ULAs (uniform linear arrays) and a 2D world assumption is used in research papers on 5G localization, so that is the model we use for explaining the array response vectors, beamforming, channel model and received signal model.

1.4.1 Related Documents

Unless otherwise indicated, source material on the formulas, definitions and concepts in this subsection can be found in the following textbooks: [4, 5, 6].

1.4.2 Angle of Arrival (AoA)

Given a signal travels along a path from a transmitter to a receiver, the angle of arrival is the relative angle between the receiver and the path at the point it meets the receiver. See Figure 1.

1.4.3 Angle of Departure (AoD)

Given a signal travels along a path from a transmitter to a receiver, the angle of departure is the relative angle between the transmitter and the path at the point it starts at, at the transmitter. See Figure 1.

1.4.4 Time of Arrival (TOA)

Time of arrival is the time at which a signal is received by a receiver.

1.4.5 Gain

Gain, when used for antennas, is defined as the "ratio of the radiation intensity, in a given direction, to the radiation intensity that would be produced if the power accepted by the antenna were isotropically radiated" [7]. Gain can be used not just for transmitted signals, but also received signals. In the previous definition, 'radiation intensity' is the electromagnetic power either transmitted or received by the antenna. For something to be isotropically radiated means the intensity of the radiation

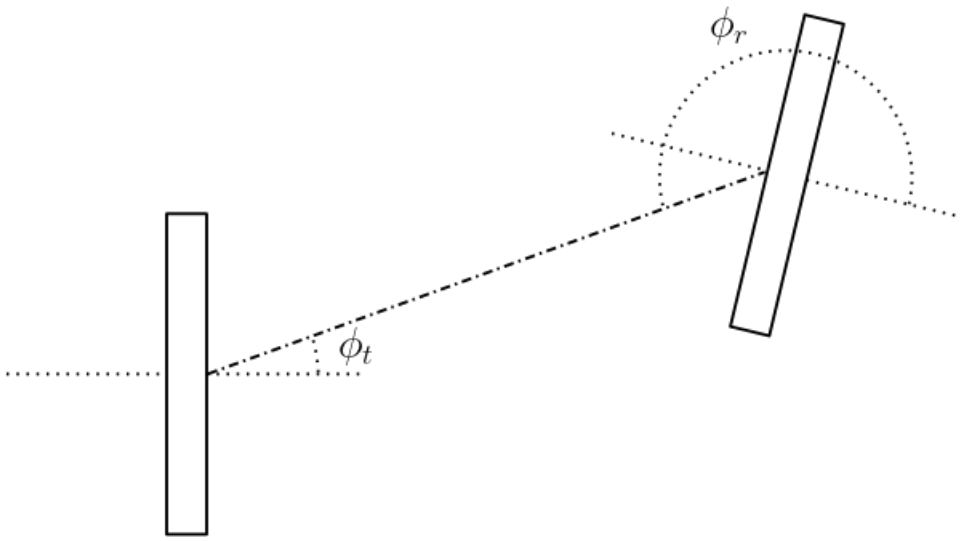

Figure 1: A diagram illustrating AOD, denoted as ϕ_t, and AOA, denoted as ϕ_r. The dash-dotted line is the LOS path the signal travels along, the dotted circular arcs indicate the angles for the AOD and AOA. The solid rectangles are the BS and MS, and the dotted lines on either side of them are perpendicular to them, indicating the reference to which AOA and AOD angles are measured.

is equal in all directions. Gain is a unitless value, and is often expressed using decibels.

1.4.6 Friis Transmission Equation

The Friis transmission equation is defined as:

$$\frac{P_r}{P_t} = G_t \cdot G_r \left(\frac{\lambda}{4\pi \cdot d}\right)^2 \tag{1}$$

where G_t and G_r is the gain at the transmitter and receiver respectively, P_t and P_r is the power transmitted and received at the transmitter and receiver respectively, λ is the wavelength and d is the distance between the transmitter and the receiver (note: d will be reused to represent the spacing between antenna elements when not being used in the Friis transmission equation). The term $\left(\frac{\lambda}{4\pi \cdot d}\right)^2$ (due to the inverse-square law, see Figure 2) models the path loss incurred on a signal as it travels through free space (i.e. a vacuum). The Friis transmission equation is useful for modelling signal strengths when attenuation from air particles does not significantly affect the results of the modelled algorithm/protocol.

1.4.7 Received Signal Strength (RSS)

The received signal strength is the power of a received signal. This can be modeled using the Friis transmission equation and solving for P_r:

$$P_r = P_t \cdot G_t \cdot G_r \left(\frac{\lambda}{4\pi \cdot d}\right)^2 \tag{2}$$

The RSS can be used for estimating the distance a signal has travelled, given all the other parameters are known. Solving for the distance gives the following equation:

$$d = \sqrt{\frac{P_t \cdot G_t \cdot G_r}{P_r}} \left(\frac{\lambda}{4\pi}\right) \tag{3}$$

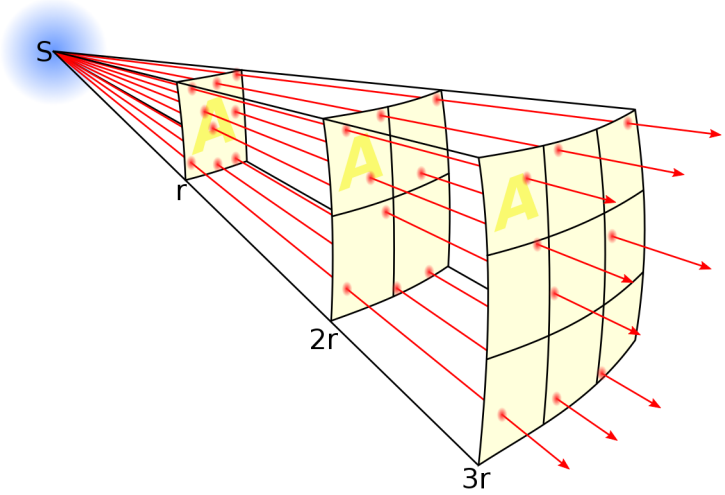

Figure 2: A figure depicting the inverse square law. With a linear increase in distance from the source of the signal, S, there is a quadratic increase in the area the power of the signal is distributed (indicated by the grids with $1^2 = 1$, $2^2 = 4$ and $3^2 = 9$ tiles). The figure was made by the 'Borb' user on Wikipedia [8], taken from the page on Inverse-square Law [9], under the GNU Free Documentation License [10], with no modifications made.

1.4.8 Uniform Linear Array (ULA)

A ULA (uniform linear array) is an antenna array where each antenna element is placed along a straight line, evenly spaced a part. This is the simplest type of MIMO antenna configuration, and it appears in 5G localization papers more often than not. Figure 3 illustrates a ULA being used for beamforming.

1.4.9 Representing Signals Using Complex Numbers

A signal is primarily characterized by a frequency as well as an amplitude. Euler's formula is incorporated into the mathematical representation of signals, as it allows for convenient mathematical operations. Euler's formula is as follows:

$$e^{i\phi} = \cos\phi + i\sin\phi$$

where ϕ is an angle expressed in radians and i is the imaginary number. For representing a signal as a function of time (AKA 'in the time domain'), the following is used:

$$A \cdot e^{j(2\pi ft+\phi)} \tag{4}$$

where A is the amplitude of the signal, f is the frequency of the signal, t is time and ϕ is the phase offset. Notice also that i was replaced with j. When working with electronics, j is used to represent imaginary numbers to avoid confusion with the symbol i for electric current. The phase offset ϕ is used for representing the relative phase differences between signals. Discarding the imaginary component of this representation gives the real component of the signal (both mathematically and literally).

Phase offsets may be represented using $e^{j\phi}$, where ϕ is the angle to offset a given frequency by. Here is an example of changing a signal's phase offset using the complex number representation for signals:

$$A \cdot e^{j(2\pi ft+\phi_0)}e^{j\phi_1} = A \cdot e^{j(2\pi ft+\phi_0+\phi_1)}$$

Originally the signal, represented by $A \cdot e^{j(2\pi ft+\phi_0)}$, had an offset of ϕ_0, but the phase shift incurred by $e^{j\phi_1}$ makes it now have an offset of $\phi_0 + \phi_1$.

1.4.10 Complex Gain

Complex gain is like gain, but incorporates an additional phase shift. It may be expressed similar to Equation (4), possibly with different variable names to avoid confusion. The complex gain can be expressed as:

$$G \cdot e^{j\phi} \tag{5}$$

where G is the gain, and ϕ is the phase shift.

1.4.11 Subcarriers

5G communications utilize a multiplexing scheme called OFDM. OFDM allows for higher data rates by enabling a transmitter to transmit overlapping (in the time and space domain) frequencies which are orthogonal to each other that can be separated and read individually by a receiver. Each of these frequencies is called a 'subcarrier', and they are each used to transmit symbols in parallel, thus increasing data rates. At the receiver end, a fast Fourier transform is used to separate the individual frequencies and read the symbols carried over each subcarrier. Given a bandwidth B and number of subcarriers N, there will be N subcarriers each assigned a frequency within the bandwidth B for performing OFDM.

1.4.12 Array Response Vectors

Array response vectors describe the relative phase differences between each signal being transmitted (or received) from each antenna element based off of the AOD (or AOA). As a result, they can be defined in many different ways. For a ULA, the array response vector for the transmitter can defined as such [11]:

$$\begin{aligned}\mathbf{a}_t\left(\phi_t\right) = \frac{1}{\sqrt{N_t}}\Big[1, e^{j\frac{2\pi}{\lambda}d\sin(\phi_t)}, e^{j2\frac{2\pi}{\lambda}d\sin(\phi_t)}\ldots \\ \ldots, e^{j(N_t-2)\frac{2\pi}{\lambda}d\sin(\phi_t)}, e^{j(N_t-1)\frac{2\pi}{\lambda}d\sin(\phi_t)}\Big]^T\end{aligned} \tag{6}$$

Equivalent representations include [12]:

$$\mathbf{a}_t(\phi_t) = \frac{1}{\sqrt{N_t}}\Big[1, e^{-j\frac{2\pi}{\lambda}d\sin(\phi_t)}, e^{-j2\frac{2\pi}{\lambda}d\sin(\phi_t)}\ldots \\ \ldots, e^{-j(N_t-2)\frac{2\pi}{\lambda}d\sin(\phi_t)}, e^{-j(N_t-1)\frac{2\pi}{\lambda}d\sin(\phi_t)}\Big]^T \tag{7}$$

and [13]

$$\mathbf{a}_t(\phi_t) = \frac{1}{\sqrt{N_t}}\left[e^{-j\left(\frac{N_t-1}{2}\right)\frac{2\pi}{\lambda}d\sin(\phi_t)}, e^{-j\left(\frac{N_t-3}{2}\right)\frac{2\pi}{\lambda}d\sin(\phi_t)}\ldots \right. \\ \left. \ldots, e^{j\left(\frac{N_t-3}{2}\right)\frac{2\pi}{\lambda}d\sin(\phi_t)}, e^{j\left(\frac{N_t-1}{2}\right)\frac{2\pi}{\lambda}d\sin(\phi_t)}\right]^T \tag{8}$$

Where λ is the wavelength of the signal, d is the spacing between antenna elements, N_t is the number of antenna elements and ϕ_t is the AOD of the transmitted signal. The receiver's array response vector for each of the previous definitions is given by replacing N_t with N_r, $\mathbf{a}_t$ with $\mathbf{a}_r$, and ϕ_t is replaced with ϕ_r to define the AOA of the received signal. The n^{th} element in the array response vector corresponds to the n^{th} antenna element in the ULA. A given element in the array response vector corresponds to the phase shift incurred on the signal transmitted (or received) from (or at) the corresponding antenna element due to the parameters ϕ, d and λ.

These array response vectors model the phase difference assuming that the signal is in the far-field. What that means is that the wavefront of the signal at the receiver can be locally approximated as a straight line due to travelling a significant distance. In 3D, this line would instead be a plane.

The $d\sin(\phi)$ term is the extra distance the signal from an antenna element's neighbouring antenna element must travel due to the angle ϕ. The $\frac{2\pi}{\lambda}$ term is for converting the distance $d\sin(\phi)$ into the incurred phase shift.

The definition in (6) results in the topmost element of the vector corresponding to the topmost element of the ULA (when oriented vertically). The definition in (7) results in the topmost element of the vector corresponding to the bottommost element of the ULA (when oriented vertically). The definition in (8) is equivalent to the definition in (6) multiplied by a constant term $e^{-j\left(\frac{N_t-1}{2}\right)\frac{2\pi}{\lambda}d\sin(\phi_t)}$. All the definitions include a normalizing $\frac{1}{\sqrt{N_t}}$ term making the vector have a magnitude equal to 1.

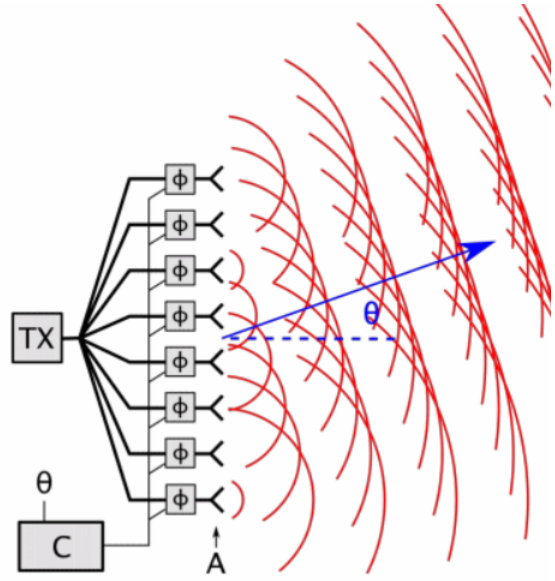

Figure 3: A figure depicting classical beamforming using a ULA. The steering angle θ along with the corresponding vector pointing in the steering direction is shown. The signals emitted from each antenna element are depicted by the red semicircles. The semicircles depict a peak of the signal.

1.4.13 Channel Model

The channel matrix $\mathbf{H}[n]$ (also called the channel model) models the relative phase shift and absolute gain a signal using subcarrier n travelling from antenna t of the transmitter to antenna r of the receiver undergoes via the entry $\mathbf{H}[n]_{r,t}$. Let N_t and N_r be the number of antenna elements at the BS and MS respectively. Assuming only LOS propagation, the resulting $N_r \times N_t$ matrix which models the channel from the transmitter to the receiver is:

$$\mathbf{H}[n] = \mathbf{a}_r(\phi)\sqrt{N_t N_r}\frac{h}{\sqrt{\rho}}e^{\frac{-j2\pi n\tau}{NT_S}}\mathbf{a}_t(\phi)^H \tag{9}$$

where h is the complex channel gain, ρ is the path loss and the term $e^{\frac{-j2\pi n\tau}{NT_S}}$ is the phase change due to the TOA τ. In the term $e^{\frac{-j2\pi n\tau}{NT_S}}$, N is the number of subcarriers, n is the given subcarrier and T_s is the sampling period (which is the inverse of the bandwidth B). The term $\frac{n\tau}{NT_S} = \frac{n\tau B}{N} = \frac{n}{N}B\tau$ in the exponent resolves to the number of cycles a signal with frequency $\frac{n}{N}B$ goes through while travelling from the transmitter to the receiver (assuming the transmitter and receiver are approximated as single antenna elements). Another appropriate representation of the term $e^{\frac{-j2\pi n\tau}{NT_S}}$ for the purpose of modelling a channel is $e^{-j2\pi f\tau}$, where f is the frequency of the signal. This would be more in-line with the definition of the array response vectors.

As mentioned, the previously described channel model assumes only LOS. To incorporate signals transmitted from multiple paths, due to NLOS transmission, the model must be modified slightly. In [11] this is done using a summation. An equivalent representation in [13] is given by stacking array response vectors into matrices. Let K denote the number of combined LOS and NLOS paths, which are indexed from 0 to $K-1$ such that 0 is the LOS path and all other values are NLOS paths. The channel model assuming multipath is defined as follows:

$$\mathbf{H}[n] = \mathbf{A}_r[n]\Gamma[n]\mathbf{A}_t^{\mathrm{H}}[n] \tag{10}$$

where the array response vectors are stacked to form $\mathbf{A}_t[n]$ and $\mathbf{A}_r[n]$ like such:

$$\begin{aligned} \mathbf{A}_t[n] &= \left[\mathbf{a}_{t,n}\left(\phi_{t,0}\right), \ldots, \mathbf{a}_{t,n}\left(\phi_{t,K}\right)\right] \\ \mathbf{A}_r[n] &= \left[\mathbf{a}_{r,n}\left(\phi_{r,0}\right), \ldots, \mathbf{a}_{r,n}\left(\phi_{r,K}\right)\right] \end{aligned} \tag{11}$$

The AOD and AOA for the LOS path is denoted by $\phi_{t,0}$ and $\phi_{r,0}$ respectively, and all other values of k denote the angles $\phi_{t,k}$ and $\phi_{r,k}$ for NLOS paths. The matrix $\Gamma[n]$ in Equation 10 is defined as:

$$\begin{aligned} \Gamma[n] &= \sqrt{N_t N_r} \\ &\times \operatorname{diag}\left\{\frac{h_0}{\sqrt{\rho_0}} e^{\frac{-j2\pi n\tau_0}{NT_s}}, \ldots, \frac{h_K}{\sqrt{\rho_K}} e^{\frac{-j2\pi n\tau_K}{NT_s}}\right\} \end{aligned} \tag{12}$$

where τ_k, h_k and ρ_k denotes the TOA, complex channel gain and path loss of the k^{th} path respectively.

1.4.14 Beamforming

Beamforming allows for many benefits in 5G communications, such as spatial multiplexing and increasing the signal-to-noise ratio and range of a given signal. Beamforming is the process of transmitting (or receiving) the same signal from multiple antenna elements, but with amplitude and phase offsets assigned to each individual antenna element so that a specific 'radiation pattern' is formed. The radiation pattern indicates the gain of signal as a function of the angle that it is transmitted (or received) from (or at). The radiation pattern is typically meant to be a 'beam' which focuses the power of the signal in a specific direction. Typically the spacing between the antenna elements, d, is between 0.5λ and λ where λ is the wavelength of the frequency transmitted. Going largely outside of these boundaries results in ineffective beamforming. Figures 4 and 5 show examples of radiation patterns and how more antenna elements allow for narrower beams. Additionally, it is seen that the intended beam, called the main lobe, has a 'mirrored' identical and unintended beam, called the rear lobe. Rear lobes and main lobes come in different shapes and sizes for different beamforming patterns and antenna configurations.

This subsubsection will explain a particular type of beamforming called 'classical beamforming'. Classical beamforming solely aims to maximize the gain in a specified direction. Figure 3 illustrates the phase shifts at each

antenna element when classical beamforming. A beamforming weight vector is what specifies the amplitude changes and phase offsets of the signal at each antenna element. For classical beamforming, the beamforming weight vector is very similar to the array response vector. It is defined as:

$$\mathbf{w}(\theta) = \left[1, e^{-j\frac{2\pi}{\lambda}d\sin(\theta)}, e^{-j2\frac{2\pi}{\lambda}d\sin(\theta)} \dots \right. \\ \left. \dots, e^{-j(N-2)\frac{2\pi}{\lambda}d\sin(\theta)}, e^{-j(N-1)\frac{2\pi}{\lambda}d\sin(\theta)}\right]^T \tag{13}$$

when corresponding to the array response vector definition in Equation (6). The only newly introduced variable shown in Equation (13) is θ, which indicates the direction the beam is formed in. For classical beamforming, $d = \frac{\lambda}{2}$ ideally.

To measure the gain of the signal transmitted by the ULA as a function of the AOD, the following formula is used:

$$G_t(\phi_t, \theta_t) = \left|\mathbf{a}_t(\phi_t)^T \mathbf{w}(\theta_t)\right|^2 \tag{14}$$

where ϕ_t is the AOD. For measuring the gain of the signal received by the ULA as a function of the AOA, the following equation is used:

$$G_r(\phi_r, \theta_r) = \left|\mathbf{a}_r(\phi_r)^T \mathbf{w}(\theta_r)\right|^2 \tag{15}$$

which is the same as Equation 14 but with the subscripts changed to indicate it is for the receiver.

Beamforming is a type of precoding. The classical beamforming algorithm can be carried out using an analog beamforming architecture. Using a digital beamforming architecture allows for modifying the amplitude and phase offset of 2 or more signals being transmitted from each antenna element simultaneously, so that more than one beam can be formed simultaneously. Not all MIMO hardware is capable of digital beamforming as it is more costly to implement, and in most scenarios only benefits the BS. Digital beamforming can used for the BS to serve multiple different MSs at the same time, where each MS is assigned a beam. Instead of a beamforming weight vector, something called a precoding matrix is used to represent the the phase shifts and amplitudes of the digital beamformer.

Precoding matrices are frequently defined as:

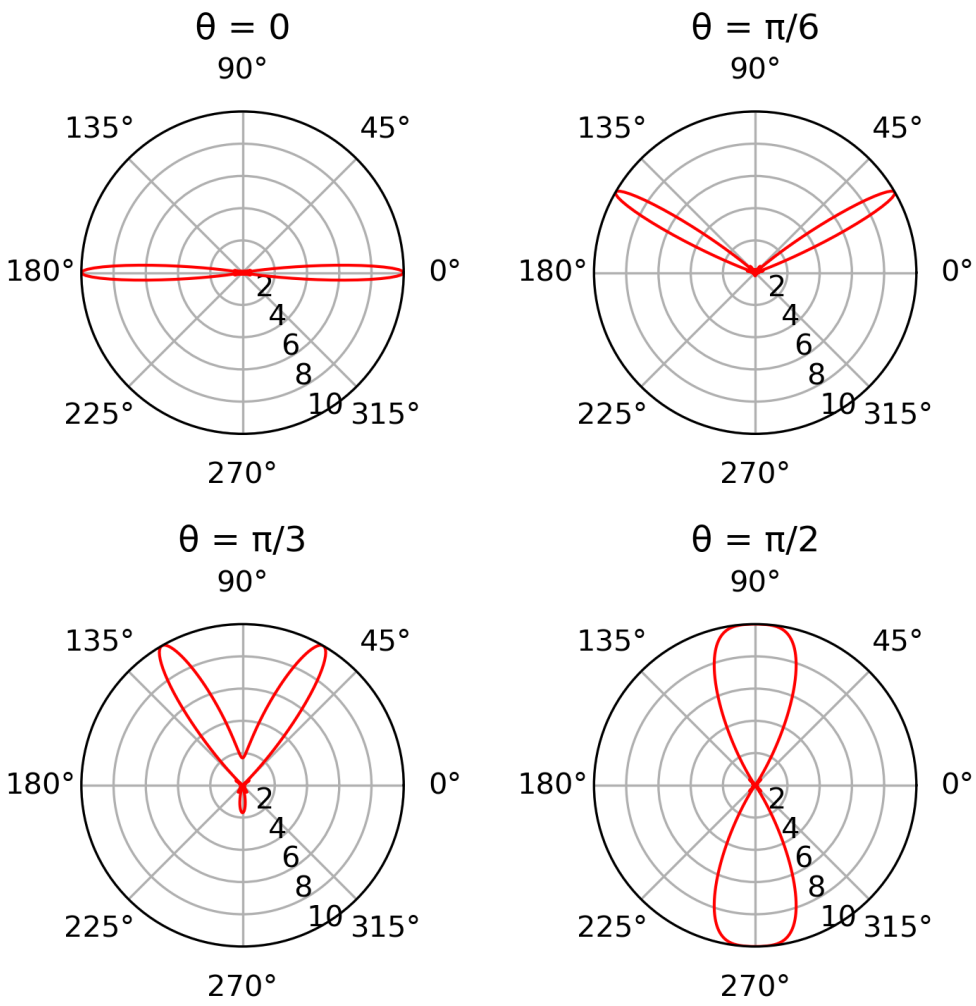

Figure 4: Polar plots depicting the radiation pattern from classical beamforming using a ULA with 10 antenna elements. The steering angle θ is depicted above each plot. The frequency of the signal is set to 25 GHz, corresponding to a wavelength of $\lambda = 11.992$ millimeters. The antenna elements are spaced $d = \frac{\lambda}{2} = 5.996$ millimeters a apart.

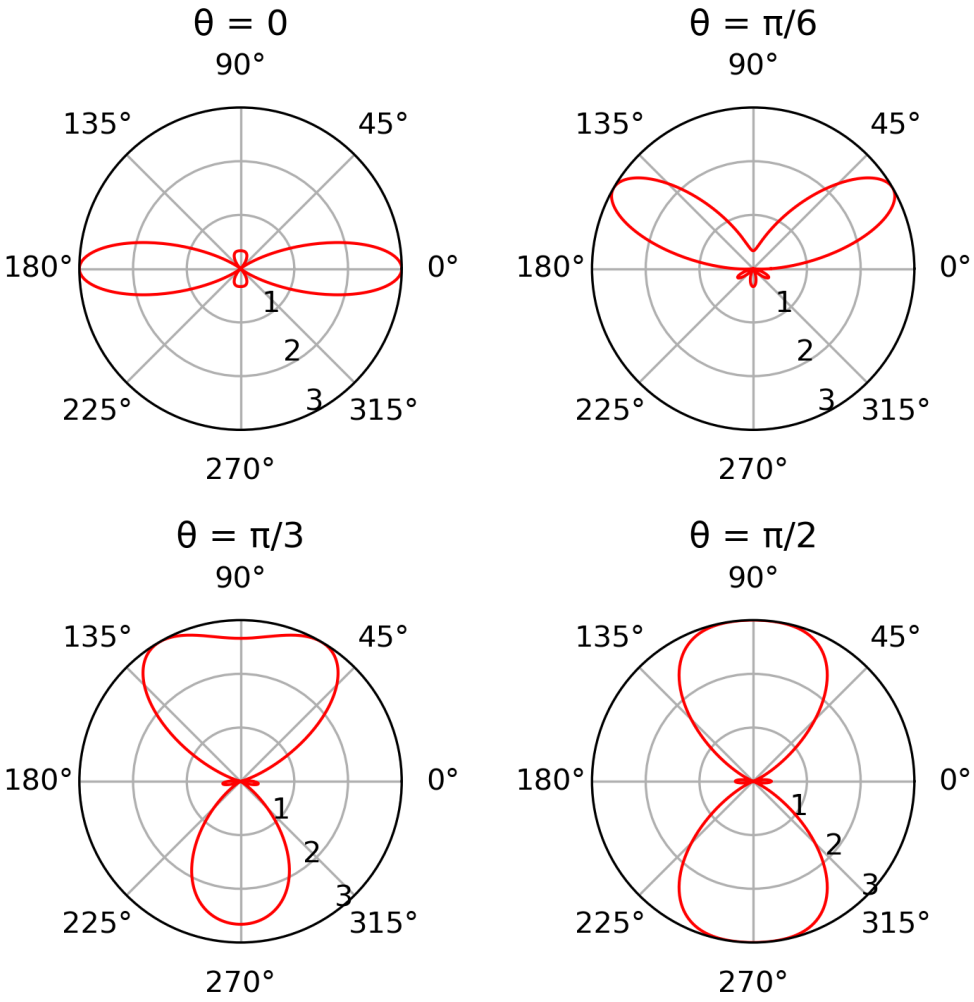

Figure 5: Polar plots depicting the radiation pattern from classical beamforming using a ULA with 3 antenna elements. The steering angle θ is depicted above each plot. The frequency of the signal is set to 25 GHz, corresponding to a wavelength of $\lambda = 11.992$ millimeters. The antenna elements are spaced $d = \frac{\lambda}{2} = 5.996$ millimeters a apart.

$$\mathbf{F}[n] \in \mathbb{C}^{N_t \times M_t}$$

where N_t denotes the number of transmit antenna elements and M_t denotes the number of simultaneously transmitted signals (usually referred to as symbols) and n denotes the subcarrier. The parameter n determines the frequency, and subsequently the λ used for calculating relative phase shifts in each entry of the matrix. Each column of the precoding matrix can be seen as a beamforming weight vector which changes the phase and amplitude of a corresponding symbol that is transmitted (or received) from (or at) all the antenna elements.

1.4.15 Received Signal Model

Let $\mathbf{n}[n] \in \mathbb{C}^{N_r}$ be a normally distributed noise vector and let $\mathbf{x}[n] \in \mathbb{C}^{M_t}$ be the symbols that are simultaneously transmitted via the digital beamformer using subcarrier n. Using $\mathbf{H}[n] \in \mathbb{C}^{N_r \times N_t}$ from Equation (9), the received signal can be expressed as:

$$\mathbf{y}[n] = \mathbf{H}[n]\mathbf{F}[n]\mathbf{x}[n] + \mathbf{n}[n] \tag{16}$$

resulting in $\mathbf{y}[n]$ being a vector of length N_r, corresponding to the signal received at each of the receiver's antenna elements.

Additionally, when modelling multiple transmissions (across the time domain), a transmission may be denoted using a subscript such as g, like so:

$$\mathbf{y}^{(g)}[n] = \mathbf{H}[n]\mathbf{F}^{(g)}[n]\mathbf{x}^{(g)}[n] + \mathbf{n}^{(g)}[n] \tag{17}$$

where g denotes one of G sequential transmissions from 0 to $G-1$. Note that there isn't a subscript on the channel matrix, as it is assumed that the channel stays constant during the G transmissions. The G transmissions may be a known sequence of symbols that the receiver is expecting to receive (but don't necessarily need to be).

1.4.16 Localization Using Channel Estimation

Channel estimation is the process of gaining channel state information (CSI) of the channel going from a transmitter and receiver. The CSI can

consist of many different properties. The channel model presented in this document is parameterized using AOA, AOD, path loss, gain and TOA. The parameters of the channel model are what correspond to the CSI properties. That means, if a channel estimation process is utilizing a channel model parameterized using AOA, AOD, path loss, gain and TOA, then the CSI consists of those parameters (AOA, AOD, path loss, gain and TOA). The channel model presented in this document is thus ideal for channel estimation techniques aiming to perform localization.

Channel estimation typically falls into 2 common paradigms: least squares approaches and compressed sensing (CS) approaches. Compressed sensing channel estimation is particularly common in 5G communications as it makes use of the angular sparsity of 5G channels. That is, 5G channels typically have low amounts of multipath components compared to the bandwidth and number of antennas used. The compressed sensing can be formulated by taking the geometric channel model (as presented in this document) and converting it to the 'beamspace' representation. The beamspace representation makes explicit the angular sparseness due to low amounts of multipath components. Other techniques may be used alongside compressed sensing to refine the estimate of the localization. More info on these channel estimation techniques can be found at [14]. Two implementations of localization which use compressed sensing are described in [13] and [12].

1.4.17 Localization Using Beam Switching

Localization using beam switching is also sometimes referred to as localization using beam steering. Beam switching is typically the process of changing beams to increase the quality of a channel between a BS and a moving MS. Beam switching can also be use for localization, by changing the direction of the beam(s) (at the BS or the MS, or both) and using the RSS of each beam position to pinpoint the location of the MS. A simple and practical algorithm for performing this would be to 'sweep' the beam in a full 360 degrees, and take the beam with the highest RSS as the AOA (or AOD), and use the RSS to determine the distance the MS is away from the BS.

1.5 Application

The algorithms explained in this document are applicable in a wide variety of scenarios. One of the most important use cases may be the syngergy between localization and communications. With better localization, comes better beam forming and thus improved communications. Localization can provide information on how to more accurately direct beams. The inverse can also hold true, beamforming can provide information on localization, as presented in this document.

Localization using 5G can be applied to a variety of use cases pertaining to smart factories [15]. These use cases include:

1. monitoring and locating assets such as storage in a warehouse
2. monitoring and locating tools, especially useful for modular assembly lines
3. controlling autonomous forklifts for moving and lifting heavy assets
4. controlling autonomous robots for delivering goods and/or tools to and from assembly lines
5. facilitating augmented reality which can be used to develop prototypes of products or help train staff

Other use cases outside of the smart factory include [16]:

1. relative positioning between autonomous vehicles, for cooperative tasks such as truck platooning or for aiding in collision avoidance
2. augmented reality in a more general sense
3. drone navigation and positioning
4. accurate positioning for emergency situations such as 911 calls

2 Functional Overview

2.1 System Overview

Our implementation consists of 4 core components.

1. The channel estimation implementation.
2. The classical beamforming implementation.
3. The beam switching localization combined with channel estimation localization.
4. Code for running experiments.

We chose Python for our implementation. The channel estimation algorithm is implemented using the method described in [13].

2.2 Assumptions

2.2.1 Antenna Hardware

We assume all antenna elements are isotropic. We also assume that each antenna array has at least one antenna element that can measure received signal strength. This is not an unreasonable assumption, as it has been made before [17] and also been demonstrated [18].

2.2.2 Mobile Station Velocity

We assume the mobile station has a negligible velocity in comparison to the time it takes to estimate its position. Our main reference of interest makes the same assumption.

2.2.3 Line of Sight

doc It is assumed that there is line of sight between the base station and mobile station. That is, the straight line path that passes through both stations is free of physical obstructions that would stop a signal travelling along that path.

3 Detailed Functional Descriptions

3.1 Channel Estimation Localization

In this simulation, we implemented the Channel Estimation Localization described in [13] using Python. The implementation explores two parameters: the 5G wave length λ and the spacing distance d between each antenna in ULA.

The goal of this simulation is to explore how changing the wave length λ and the spacing distance d can affect the accuracy of the estimation of the location.

3.1.1 Algorithm

The goal of the algorithm is to estimated the location and orientation of MS from respect of BS's location and orientation. As mentioned in Section 1.4.13, the localization in this algorithm is done by applying CSI. Hence, the first step in this algorithm is to compute the channel matrix $H[n]$. To do so, the simulation starts with computation of stacked array response vectors $\mathbf{A}_t[n]$ and $\mathbf{A}_r[n]$ using equation 11 and equation 8. The channel model $H[n]$ is computed based on equation 10 using the stacked array response vectors $\mathbf{A}_t[n]$ and $\mathbf{A}_r[n]$.

Next step is to compute the received signal model 1.4.15 $y^{(g)}[n]$ using equation 17. In this simulation, since only one symbol is transmitted, $x^{(g)}[n]$ is omitted.

When the received signal model $y^{(g)}[n]$ computed, the following steps are to estimate the position $\hat{p}$ and orientation $\hat{\alpha}$ of the MS using $y^{(g)}[n]$.

First, the virtual spatial angles vectors U_{Tx}, U_{Rx} are created by formulas from [13] as following:

$$\mathbf{U} \triangleq [\mathbf{u}(-\frac{(N_t-1)}{2}), ..., \mathbf{u}(\frac{(N_t-1)}{2})] \tag{18}$$

$$\mathbf{u}\,(p) \triangleq [e^{-j2\pi\frac{N_t-1}{2}\frac{p}{N_t}}, ..., e^{j2\pi\frac{N_t-1}{2}\frac{p}{N_t}}]^T \tag{19}$$

where N_t is assumed to be even.

Then the approximately sparse vector $\hat{h}[n]$ is computed using the equation 36 from [13]:

$$\hat{\mathbf{y}}[n] = \mathbf{\Omega}[n]\hat{\mathbf{h}}[n] + \hat{\mathbf{n}}[n] \tag{20}$$

where $\hat{y}[n]$ is our received signals. In this simulation, we assume it is $y^{(g)}[n]$. Also, the $\Omega[n]$ is the sensing matrix defined by [13] as following:

$$\mathbf{\Omega}[n] = \begin{bmatrix} \mathbf{\Omega}^{(1)}[n] \\ \vdots \\ \mathbf{\Omega}^{(G)}[n] \end{bmatrix} \tag{21}$$

where $\Omega^{(g)}[n]$ is

$$\mathbf{\Omega}^{(g)}[n] = (\mathbf{U}_{Tx}^{H}\mathbf{F}^{(g)}[n]\mathbf{x}^{(g)}[n])^{T} \otimes \mathbf{U}_{Rx} \tag{22}$$

However, as mentioned in equation 16 and equation 17, $n[n]$ is the normally distributed noise vector. Hence, simply perform a division between $\hat{y}[n]$ and $\Omega[n]$ will not give the $\hat{y}[n]$. Therefore, a modified distributed compressed sensing simultaneous orthogonal matching pursuit (DCS-SOMP) as proposed as Algorithm 1 in [13] is applied. During the execution of this algorithm, the estimated AOD $\hat{\theta}_{Tx,0}$ and the estimated AOA $\hat{\theta}_{Rx,0}$ for LOS path is computed as well. Same applied for estimated AOD $\hat{\theta}_{Tx,t}$ and the estimated AOA $\hat{\theta}_{Rx,t}$ for NLOS path are computed as well.

Once $\hat{y}[n]$ is computed, the estimated distance between MS and BS in LOS path can be computed by:

$$\hat{d} = \overset{argmax}{t_k} \; c|\mathbf{a}^{H}(t_k)\hat{\mathbf{h}}^{(k)}|^2 \tag{23}$$

for each path $k = 0, ..., K$ where K is the total number of paths (including both LOS and NLOS paths), and c is the speed of light.

Finally, the estimated position $\hat{p}$ and orientation $\hat{\alpha}$ are computed as following:

$$\hat{\mathbf{p}} = \mathbf{q} + \hat{d}[cos(\hat{\theta}_{Tx,0}), sin(\hat{\theta}_{Rx,0})] \tag{24}$$

$$\hat{\alpha} = \pi + \hat{\theta}_{Tx,0} - \hat{\theta}_{Rx,0} \tag{25}$$

where q is the location of BS, which is assumed to be the center $(0, 0)$.

3.1.2 Results

To allow us to run the algorithm with different wave length λ and the spacing distance d between each antenna in ULA. We rigged the implementation so that it takes two parameters, d and λ, and run the algorithm against random scatters and random MS location.

Then, we created a list of experiment parameter tuples. A experiment parameter tuple simply contains a predefined wave length λ and the spacing distance d. The list of tuples are created as following, where c is the light of speed.

Algorithm 1 Create a list of experiment parameter tuples

```
1: Freqs = [24GHz, 32GHz, 37GHz, 41GHz, 46GHz, 51GHz, 66GHz, 81GHz]
2: Wavelengths = Freqs / c
3: RelativeLengths = [0.25, 0.333, 0.5, 0.75, 1.0, 1.5, 2.0]
4: set = ∅
5: for each λ ∈ Wavelengths do
6:     for each l ∈ RelativeLengths do
7:         d = λl
8:         set += (d, λ)
9:     end for
10: end for
11: return set
```

Using this setup, we have $8 * 7$ in total 56 experiments with each wave length λ and each spacing distance d. Then for each experiment, we ran the algorithm 5 times and calculated the mean and 95% confidence interval of the localization error and the orientation error. The localization error is the error between the estimated position and the actual position of the MS, and the orientation error is the error between the estimated orientation and the actual orientation of the MS.

Once we finished all the experiments from the list of experiment parameter tuples, we plot several line plots as shown in Algorithm 2 below. This code gave us 2 plots for each wave length λ, in total 16 plots.

Plots are stored in the directory called "fifth experiments" in the submitted code base. We didn't put them in this report due to the large amount

Algorithm 2 Plot the simulation results

Require: Results = all simulation results

1: **for each** $\lambda \in \mathcal{W}avelengths$ **do**
2: subResults = {$\forall$ result *in* Results | result is experiemented with wavelength λ}
3: plot the localization error vs d for this particular λ
4: plot the orientation error vs d for this particular λ
5: **end for**

of figures produced.

As for results, unfortunately, we didn't find any meaningful relationship between the accuracy of estimation and wave length λ or the spacing distance d between each antenna in ULA. Originally, we had the expected simulation result that the accuracy of the estimation might be a linear relationship with λ/d or d/λ, since the formula of array response vectors in equation 8 contains d/λ. However, it turns out that our implementation has a large random localization and orientation errors such that it could hides the relationship we are trying to find. Despite a large amount of time spent on debugging, we were still far from the expected simulation result.

3.2 Combining Channel Estimation Localization and Beam Switching Localization

3.2.1 Algorithm

We propose a method for combining beam switching localization and channel estimation localization. Other ideas on how to combine these two methods are discussed in Section 4 (we did not have the time to explore these other avenues and encountered some roadblocks).

As seen in Figures 4 and 5, the beam pattern for classical beam forming is symmetrical when assuming isotropic antennas. There is a main lobe and an equivalent rear lobe. A beam pattern such as this one is less than ideal when performing beam switching localization as it is difficult to distinguish between the main lobe and the rear lobe when performing RSS measurements. As a result, we propose a simple algorithm for harnessing

the advantages of both methods of localization. The steps of algorithm are listed in Algorithm 3 with an accompanying diagram in Figure 6.

The general idea of the algorithm is to first perform channel estimation localization as a 'rough guess' of where the BS is. Then, a more accurate beam switching localization is used to pinpoint where the BS is more precisely. Instead of doing a full beam sweep, the beam switching algorithm first sweeps m_b number of beams around the initial estimate of the BS given by channel estimation localization. If the beam switching localization agrees enough with the channel estimation localization (within a certain threshold) then the algorithm returns the beam switching localization result. The benefit of this is that the algorithm won't have to shoot out every single beam every single time it executes; it can just focus on the beams that are close to the initial channel estimation guess.

Algorithm 3 Beam Switching and CSI Localization(s_b,m_b,t)

1: BS and MS perform initial channel estimation localization
2: BS forms m_b subsequent beams, with the middle of the beams aimed at the initial channel estimation localization, with s_b radians as the spacing between each of the beams
3: MS measures the RSS of each of the BS's formed beams
4: MS determines the 2 possible beams belonging to the strongest RSS
5: MS picks the beam which gives a localization most similar to the channel estimation localization
6: let d_e be the estimated distance of the MS from the BS based off the channel estimation localization
7: let d_b be the estimated distance of the MS from the BS based off the beam switching localization
8: **if** $d_b > d_e \cdot t$ **then**
9: repeats steps 1 to 7, but with $m_b = \frac{2\pi}{s_b}$ and return the beam switching localization result
10: **else**
11: return the beam switching localization result
12: **end if**

The benefit to using classical beamforming is that it has very narrow beams. The HPBW (half-power beam width) of a beam is the width of a

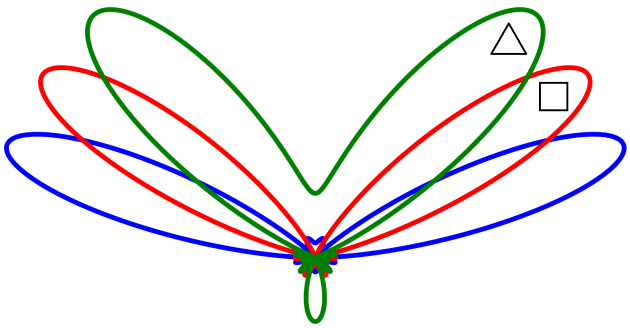

Figure 6: A figure showing the beam switching and channel estimation localization methods working together. The initial channel estimation is indicated by the square. The beam switching shoots out $m_b = 3$ beams, with the center beam (in red) directed at the square. The actual position of the BS is indicated by the triangle. The RSS measurement from one of the beams (in green) directed at the triangle will give an improved localization result without having to shoot out beams in every single direction.

beam (in radians) that is at least half its maximum gain. The HPBW using classical beamforming and a ULA can be approximated as $\frac{1.78}{N_t}$ radians when $d = \frac{\lambda}{2}$, where N_t is the number of antenna elements [19]. Given an accurate-enough initial guess using channel estimation localization, a smaller amount of beams is used when performing beam-switching localization.

What makes this method of using beams and channel estimation to localize so practical, is that beams that are formed for communications can additionally be used for localization. The idea here is that the channel estimation localization is a way to get an initial estimate on the location of the BS, followed by a refinement using beam switching. If the MS wishes to communicate with the BS while moving, the beam switching localization process can continue to ensure localization and high quality communications via beamforming. If the beam switching process at some point fails to keep track of the MS's location, a channel estimation localization may be performed to relocate the MS and repeat the execution of the algorithm previously described. Thus, continued localization and high quality communications between the BS and MS.

3.2.2 Results

The algorithm described in 3.2.1 was implemented and tested using a Python implementation. Assuming a reasonable amount of noise on the RSS measurement, the localization results seem quite promising. Even with a poor initial guess from the channel estimation localization, the beam switching reliably refines the estimate. The spacing between the beams was set to the HPBW: $\frac{1.78}{N_t}$, with $N_t = 32$.

To illustrate the effectiveness of the algorithm, we setup the channel estimation algorithm so that it had a poor initial estimation of 4.71 ± 0.48 meters, and then refined it using a better beam switching localization. The BS was placed randomly between 1 and 5 meters away. The experiment was ran 500 times with results given on a 95% confidence interval. The spacing for the beams was set to $s_b = 0.0278$ radians based off the HPBW. This means there were $\frac{2\pi}{0.0278} = 113$ beams to form when doing a full beam sweep. With some fine-tuning, the parameters were set to $t = 6$ and $m_b = 50$.

For a one-to-one comparison, Algorithm 1 (using the parameters previously listed) was put up against a modified Algorithm 1, where m_b was always set to 113, and t was set to infinity. This means that the modified algorithm would always return on line 11, and our beam switching refinement strategy based off the threshold t was not used. The results are as follows: Algorithm 1 had an average positioning error of 2.74 ± 0.19, and the modified Algorithm 1 had an average positioning error of 2.79 ± 0.18. Algorithm 1 on average formed 71.47 ± 3.89 beams, and the modified Algorithm 1 (of course) on average formed 113 beams. This means that the proposed beam-refinement strategy effectively reduced the amount of beams needed to be formed, while maintaining the accuracy of the localization given by the normal beam switching algorithm.

4 Conclusion

4.1 Discussion on Previous Localization Work

We noticed a potentially significant issue regarding the previous work on channel estimation localization [13]. When changing the beamformer in the estimation process to be a classical beamformer, the localization error became extremely high. In the original paper, their results are only evaluated using a random beamformer. We are not sure if this is 100% indicative that the algorithm does not work when using a classical beamformer, as the public implementation (as well as our Python implementation) only assumes a single symbol is sent (as opposed to a sequence). It also does not simulate changes in the SINR due to the beamformer.

Their are also some issues with the paper. It does not explain the reasoning very well for the algorithms it chose to perform localization. Instead of laying out the intuition for the algorithms used, they expect the intuition to follow from explanation of the algorithms (which are very complicated). There are also some minor issues we noticed with missing references (example: one in section 2.A 'khateeb3') and minor mistakes in a couple of definitions (example: the refer to a classical beamformer as just a 'beamformer').

4.2 Ideas for Future Work

We initially wanted to combine the beam switching localization as well as the channel estimation localization using a method such as MAP estimation. The general idea was to perform the channel estimation localization using a narrow beam, and simultaneously get a RSS reading from the beam as well a TOA readying from the channel estimation. Then, combining the two measurements using MAP estimation to (what we imagine) get a more accurate localization. As previously mentioned, the error on the channel estimation localization algorithm was concerningly high when using a classical beamformer. We weren't sure we could diagnose the problem, so we decided to explore other ways of combining beam-switching and channel estimation.

5 Appendices

5.1 Change Log

Changes made since our initial submission to Brightspace on April 5th:

1. Fixed a few minor mistakes in the intro section
2. Added a figure in the intro section for explaining AOA and AOD
3. Completed Section 3.1
4. Completely re-wrote Section 3.2
5. Added to the conclusion section
6. Modified the contributions section
7. NOTE: there may be other changes we made elsewhere that we did not mention here (we can clarify via email if needed).

5.2 Code

Our code is provided alongside this document. It was developed and tested using Python 3.8.

5.3 Contributions

5.3.1 Charles Chen's Contributions

1. Wrote Python code for channel estimation localization
2. Wrote Python code for changing the antenna spacing and frequency of channel estimation localization
3. Wrote analysis on channel estimation localization (Subsection 3.1)

5.3.2 Nicolas Perez's Contributions

1. Made all the slides for the project presentation
2. Wrote all of Section 1 (including the 5G localization tutorial) and Section 3.2 of the report
3. Wrote most of Section 4 of the report
4. Wrote half of Section 2 of the report
5. Wrote Python code for classical beam forming and beam switching localization
6. Wrote Python code for combining beam switching localization and channel estimation localization

References

[1] Henk Wymeersch, Gonzalo Seco-Granados, Giuseppe Destino, Davide Dardari, and Fredrik Tufvesson. 5g mmwave positioning for vehicular networks. *IEEE Wireless Communications*, 24(6):80–86, 2017.

[2] Henk Wymeersch. 5G Positioning Tutorial. `https://youtu.be/VKF-Xgn0O6A?t=2850`, February 2022.

[3] Fuxi Wen, Henk Wymeersch, Bile Peng, Wee Peng Tay, Hing Cheung So, and Diange Yang. A Survey on 5G Massive MIMO Localization. *Digital Signal Processing*, 94:21–28, 2019.

[4] Adrián Cardalda García, Stefan Maier, and Abhay Phillips. *Location-Based Services in Cellular Networks: from GSM to 5G NR*. Artech House, 2020.

[5] Henrik Asplund, David Astely, Peter von Butovitsch, Thomas Chapman, Mattias Frenne, Farshid Ghasemzadeh, Måns Hagström, Billy Hogan, George Jongren, Jonas Karlsson, et al. *Advanced Antenna Systems for 5G Network Deployments: Bridging the Gap Between Theory and Practice*. Academic Press, 2020.

[6] Emil Björnson, Jakob Hoydis, and Luca Sanguinetti. Massive MIMO networks: Spectral, energy, and hardware efficiency. *Foundations and Trends® in Signal Processing*, 11(3-4):154–655, 2017.

[7] IEEE. Ieee standard for definitions of terms for antennas - redline. *IEEE Std 145-2013 (Revision of IEEE Std 145-1993) - Redline*, pages 1–92, 2014.

[8] Borb. Wikipedia User: Borb. `https://commons.wikimedia.org/wiki/User:Borb`, March 2022.

[9] Wikipedia. Inverse-square Law. `https://en.wikipedia.org/wiki/Inverse-square_law`, March 2022.

[10] GNU. GNU Free Documentation License. `https://www.gnu.org/licenses/fdl-1.3.html`, March 2022.

[11] Ahmed Alkhateeb, Omar El Ayach, Geert Leus, and Robert W Heath. Hybrid Precoding for Millimeter Wave Cellular Systems with Partial Channel Knowledge. In *2013 Information Theory and Applications Workshop (ITA)*, pages 1–5. IEEE, 2013.

[12] Kunlun Li, Mohammed El-Hajjar, and Lie-liang Yang. Millimeter-Wave Based Localization Using a Two-Stage Channel Estimation Relying on Few-Bit ADCs. *IEEE Open Journal of the Communications Society*, 2:1736–1752, 2021.

[13] Arash Shahmansoori, Gabriel E Garcia, Giuseppe Destino, Gonzalo Seco-Granados, and Henk Wymeersch. Position and Orientation Estimation through Millimeter-Wave MIMO in 5G Systems. *IEEE Transactions on Wireless Communications*, 17(3):1822–1835, 2017.

[14] Waheed U Bajwa, Jarvis Haupt, Akbar M Sayeed, and Robert Nowak. Compressed channel sensing: A new approach to estimating sparse multipath channels. *Proceedings of the IEEE*, 98(6):1058–1076, 2010.

[15] NGMN Alliance. Verticals urllc use cases and requirements. *NGMN Alliance*, 2019.

[16] 3GPP. 3GPP TR 22.872: Study on Positioning Use Cases, 2018.

[17] Liang Cai, Kai Zeng, Hao Chen, and Prasant Mohapatra. Good neighbor: Secure pairing of nearby wireless devices by multiple antennas.

[18] Jacob Samuelsson. Phased array antenna element evaluation, 2017.

[19] Mark A Richards. *Fundamentals of radar signal processing*. Tata McGraw-Hill Education, 2005.